HHS Public Access

Author manuscript

Kidney Int. Author manuscript; available in PMC 2022 March 03.

Published in final edited form as:

Kidney Int. 2021 July ; 100(1): 107–121. doi:10.1016/j.kint.2021.02.025.

Annexin A1 alleviates kidney injury by promoting the resolution of inflammation in diabetic nephropathy

Liang Wu[1,2,3,4,17], **Changjie Liu**[5,6,7,8,9,17], **Dong-Yuan Chang**[1,2,3,4], **Rui Zhan**[5,6,7,8,9], **Jing Sun**[10], **Shi-He Cui**[10], **Sean Eddy**[11], **Viji Nair**[11], **Emily Tanner**[11], **Frank C. Brosius**[12], **Helen C. Looker**[13], **Robert G. Nelson**[13], **Matthias Kretzler**[11,14], **Jian-Cheng Wang**[10], **Ming Xu**[15], **Wenjun Ju**[11,14], **Ming-Hui Zhao**[1,2,3,4], **Min Chen**[1,2,3,4], **Lemin Zheng**[5,6,7,8,9,16]

[1]Renal Division, Department of Medicine, Peking University First Hospital, Beijing, China;

[2]Institute of Nephrology, Peking University, Beijing, China;

[3]Key Laboratory of Renal Disease, Ministry of Health of China, Beijing, China;

[4]Key Laboratory of Chronic Kidney Disease Prevention and Treatment (Peking University), Ministry of Education, Beijing, China;

[5]The Institute of Cardiovascular Sciences, Institute of Systems Biomedicine, School of Basic Medical Sciences, Beijing, China;

[6]Key Laboratory of Molecular Cardiovascular Science, Ministry of Education, Beijing, China;

[7]Key Laboratory of Cardiovascular Molecular Biology and Regulatory Peptides, Ministry of Health, Beijing, China;

[8]Beijing Key Laboratory of Cardiovascular Receptors Research, Beijing, China;

[9]Department of Physiology and Pathophysiology, Peking University Health Science Center, Beijing, China;

[10]Beijing Key Laboratory of Molecular Pharmaceutics and New Drug Delivery Systems, State Key Laboratory of Natural and Biomimetic Drugs, School of Pharmaceutical Sciences, Peking University, Beijing, China;

[11]Division of Nephrology, Department of Internal Medicine, University of Michigan, Ann Arbor, Michigan, USA;

[12]Department of Physiology, University of Arizona, Tucson, Arizona, USA;

[13]Chronic Kidney Disease Section, Phoenix Epidemiology and Clinical Research Branch, National Institute of Diabetes and Digestive and Kidney Diseases, National Institutes of Health, Bethesda, Maryland, USA;

Correspondence: Lemin Zheng, The Institute of Cardiovascular Sciences, Health Science Center, Peking University, 30 Xueyuan Road, Haidian District, Beijing 100191, China. Zhengl@bjmu.edu.cn; or Min Chen, Renal Division, Department of Medicine, Peking University First Hospital, 8 Xishiku Street, Xicheng District, Beijing 100034, China. chenmin74@sina.com.

[17]LW and CL contributed equally to this work.

SUPPLEMENTARY MATERIAL

Supplementary File (PDF)

[14]Department of Computational Medicine and Bioinformatics, University of Michigan, Ann Arbor, Michigan, USA;

[15]Department of Cardiology and Institute of Vascular Medicine, Peking University Third Hospital, Beijing, China;

[16]China National Clinical Research Center for Neurological Diseases, Tiantan Hospital, Advanced Innovation Center for Human Brain Protection, The Capital Medical University, Beijing, China

Abstract

Since failed resolution of inflammation is a major contributor to the progression of diabetic nephropathy, identifying endogenously generated molecules that promote the physiological resolution of inflammation may be a promising therapeutic approach for this disease. Annexin A1 (ANXA1), as an endogenous mediator, plays an important role in resolving inflammation. Whether ANXA1 could affect established diabetic nephropathy through modulating inflammatory states remains largely unknown. In the current study, we found that in patients with diabetic nephropathy, the levels of ANXA1 were upregulated in kidneys, and correlated with kidney function as well as kidney outcomes. Therefore, the role of endogenous ANXA1 in mouse models of diabetic nephropathy was further evaluated. ANXA1 deficiency exacerbated kidney injuries, exhibiting more severe albuminuria, mesangial matrix expansion, tubulointerstitial lesions, kidney inflammation and fibrosis in high fat diet/streptozotocin-induced-diabetic mice. Consistently, ANXA1 overexpression ameliorated kidney injuries in mice with diabetic nephropathy. Additionally, we found Ac2-26 (an ANXA1 mimetic peptide) had therapeutic potential for alleviating kidney injuries in db/db mice and diabetic *Anxa1* knockout mice. Mechanistic studies demonstrated that intracellular ANXA1 bound to the transcription factor NF-κB p65 subunit, inhibiting its activation thereby modulating the inflammatory state. Thus, our data indicate that ANXA1 may be a promising therapeutic approach to treating and reversing diabetic nephropathy.

Keywords

Ac2-26; annexin A1; diabetic nephropathy; proresolution

Diabetic nephropathy (DN) is one of the common microvascular complications in diabetes and is the worldwide leading cause of end-stage kidney disease. The pathogenesis of DN is not fully clear yet. Growing evidence indicates that chronic low-grade inflammation is an important feature in DN.[1,2] The failed resolution of inflammation is a major contributor to the continuous development of DN.[3] It is, therefore, imperative to find endogenous mediators that can reduce inflammation to protect against the progression of DN.

Annexin A1 (ANXA1), a 37-kDa protein, is a member of the annexin superfamily.[4] It has been demonstrated to be involved in a variety of cellular biological functions, including cell proliferation, differentiation, and apoptosis. ANXA1 ameliorates microvascular complications in type 1 diabetes, attenuates insulin resistance in experimental type 2 diabetes, and protects against the development of secondary complications.[5,6] However, the

functional role of ANXA1 in DN and whether ANXA1 could affect established nephropathy through modulating inflammatory states in DN remain largely unknown.

In this study, we assessed the levels of ANXA1 (or *ANXA1* mRNA) in kidney biopsies from DN patients and evaluated their correlation with kidney function as well as outcomes in independent cohorts. We used *Anxa1* knockout (KO) and *Anxa1* transgenic (Tg) mice to investigate the role of ANXA1 in the progression of the kidney disease in diabetic mice. Furthermore, we explored the therapeutic potential of Ac2-26, an ANXA1 mimetic peptide, in treating established DN in db/db mice as well as *Anxa1* KO mice. We also investigated the mechanism of how ANXA1 mediates kidney proresolution using a tubular epithelial cell culture model.

METHODS

Patients and samples

Clinical samples were collected from 3 individual cohorts. More details are provided in the Supplementary Methods.

Detection of ANXA1 in kidneys

Immunostaining of ANXA1 using monoclonal rabbit anti-ANXA1 antibody (ab214486; Abcam) was performed on paraffin-embedded kidney sections from Chinese cohort. Correlation studies were performed between ANXA1 and clinicopathologic parameters.

RNAscope *in situ* hybridization

RNAscope *in situ* hybridization was conducted using RNAscope BROWN kit (number 322300; Advanced Cell Diagnostics) for ANXA1 (number 465411; RNAscope Probe-Hs-ANXA1; Advanced Cell Diagnostics), according to the manufacturer's instructions.

Experimental animals

Anxa1 KO mice were purchased from Cyagen Biosciences Inc. (China), which was created by transcription activator-like effector nucleases (TALEN) methods.[7] *Anxa1*-Tg mice were purchased from Viewsolid Biotech (China). *Anxa1*-Tg mice were created in C57BL/6J with mice piggyBac Transposon method.[8] The identification results of *Anxa1* KO mice and *Anxa1*-Tg mice were presented in Supplementary Figure S1. More details are provided in the Supplementary Methods.

Male diabetic db/db (C57BL/6J-LepR$^{db/db}$) mice and their nondiabetic db/m (C57BL/6J-LepR$^{db/+}$) littermates were purchased from Department of Laboratory Animal Science, Peking University Health Science Center (Beijing, China). All animal procedures were approved by the Ethics Committee of Peking University Health Science Center, and the ethics license number is LA2011-046.

Animal studies

To determine the role of endogenous ANXA1 in a model of DN, wild-type (WT), *Anxa1* KO mice, and *Anxa1*-Tg mice were induced to develop DN with the high-fat diet (HFD) plus

streptozotocin (STZ) treatment. Ac2-26 treatment was performed on db/db mice and *Anxa1* KO mice. The details of the animal studies are provided in the Supplementary Methods.

Blood and urine examination

The concentrations of urinary and plasma ANXA1, urine albumin, urine creatinine, serum creatinine, blood urea nitrogen, blood glucose, cholesterol, and triglyceride were measured following standard protocols. More details are provided in the Supplementary Methods.

Glucose tolerance test and insulin tolerance test

The glucose tolerance test and insulin tolerance test were performed following standard protocols. More details are provided in the Supplementary Methods.

Histologic analysis

Paraffin-embedded kidney tissue sections were stained with periodic acid–Schiff solution (BA-4080B; BASO) to assess glomerular mesangial matrix expansion, sclerosis, and tubulointerstitial injury, as described previously.[9–11] Detailed protocols are described in the Supplementary Methods.

Immunohistochemistry and immunofluorescence

Detailed protocols are described in the Supplementary Methods.

Transmission electron microscopy

Electron microscopic sample handling and detection were performed by the Electron Microscopic Central Laboratory of Peking University First Hospital. Detailed protocols are described in the Supplementary Methods.

Real-time quantitative polymerase chain reaction analysis

Primers used for mRNA detection are listed in Supplementary Table S1. More details are provided in the Supplementary Methods.

Flow cytometry

Flow cytometry was performed following standard protocols. Additional details are provided in the Supplementary Methods.

Cell culture and treatment

Human immortalized proximal tubule epithelial HK-2 cells were purchased from American Type Culture Collection. Detailed treatment protocols are provided in the Supplementary Methods.

Western blot

Western blot was performed following standard protocols. Additional details are provided in the Supplementary Methods.

Coimmunoprecipitation

Coimmunoprecipitation was performed following the manufacturer's instructions. Additional details are provided in the Supplementary Methods.

Nuclear factor-κB p65 activity

Following treatment, nuclear extracts were isolated using the Nuclear Extract kit, according to the manufacturer's protocols (number 40010; Active Motif). The activity of nuclear factor (NF)-κB p65 was assessed using an enzyme-linked immunosorbent assay kit (number 43296; Active Motif).

Electrophoretic mobility shift assay

Gel shift assays were performed with the LightShift chemiluminescent electrophoretic mobility shift assay kit (number 20148; ThermoFisher Scientific). Additional details are provided in the Supplementary Methods.

Surface plasmon resonance analysis

Surface plasmon resonance measurements were performed using a Biacore T200 instrument (GE Healthcare). Detailed protocols are described in the Supplementary Methods.

Statistical analysis

Data were presented as mean ± SD or median and interquartile range, as appropriate. Analytical details are provided in the Supplementary Methods. $P < 0.05$ indicates statistically significant differences.

RESULTS

Kidney cortical ANXA1 is significantly elevated in DN

To detect ANXA1 protein levels in kidney tissues in human DN, we compared the levels of ANXA1 in kidney biopsies between DN patients and healthy controls from the Chinese cohort by immunohistochemical staining (Figure 1a; Supplementary Table S2 for cohort details). Kidney biopsies from DN patients showed more intense staining of ANXA1 in the glomeruli and tubulointerstitium than healthy controls (Figure 1b and c). Correlation analyses showed that the tubulointerstitial ANXA1 expression positively correlated with serum creatinine ($r = 0.473$, $P = 0.008$; Figure 1d), 24-hour urinary protein ($r = 0.529$, $P = 0.003$; Figure 1e), and tubulointerstitial inflammation ($r = 0.431$, $P = 0.017$). Tubulointerstitial ANXA1 also showed a negative correlation with estimated glomerular filtration rate ($r = -0.464$, $P = 0.010$; Figure 1f). The glomerular ANXA1 negatively correlated with the percentage of glomerulosclerosis ($r = -0.453$, $P = 0.012$; Figure 1g). To further validate these results, we evaluated *ANXA1* mRNA expression in an independent cohort. Consistently, *ANXA1* mRNA ($\log_2$) levels were significantly higher in patients with DN from the European Renal cDNA Biobank than those in healthy living donors in both tubulointerstitial and glomerular compartment (Supplementary Figure S2; Supplementary Table S3 for cohort details). In addition, compared with nondiabetic mice, diabetic mice demonstrated a significant increase in ANXA1 levels in kidneys (Supplementary Figure S3).

To investigate the association between ANXA1 and kidney outcomes in DN patients, we used kidney biopsy samples from a Pima Indian patient population with long-term follow-up data (Supplementary Table S4 for cohort details).[12] We found that lower level of *ANXA1* mRNA at the time of biopsy was significantly associated with an increased risk of progression to a composite end point of end-stage kidney disease or 40% decline of baseline GFR measured by iothalamate clearance (n = 49 events) during a follow-up of 9.0 ± 4.0 years (log-rank test, $P = 0.049$; Supplementary Figure S4). These data suggested that higher expression of ANXA1 may be a protective factor for DN progression.

Immunofluorescence colocalization analyses showed that ANXA1 partially colocalized with tubular epithelial cells, podocytes, mesangial cells, endothelial cells, and monocytes/macrophages in kidneys of DN patients (Figure 1h and Supplementary Figure S5). To determine the major sources of ANXA1 in renal samples, *in situ* hybridization by RNAscope was performed. In biopsy samples from patients with DN, *in situ* hybridization showed that ANXA1 was mainly expressed in parietal epithelial cells and tubular epithelial cells (Supplementary Figure S6). However, there was only a minor amount of ANXA1 expression in the biopsy samples from healthy controls.

Moreover, we measured the circulating and urinary levels of ANXA1 in DN patients, diabetes mellitus patients without kidney involvement, and healthy controls (Supplementary Table S5 for general data). The level of urinary ANXA1/creatinine in DN patients was significantly higher than that in diabetes mellitus patients without kidney involvement (5.96 ± 2.42 vs. 2.30 ± 0.76 ng/mg; $P < 0.001$) and healthy controls (5.96 ± 2.42 vs. 1.29 ± 0.62 ng/mg; $P < 0.001$; Supplementary Figure S7A). The levels of urinary ANXA1/creatinine were positively correlated with serum creatinine ($r = 0.454$, $P = 0.012$) and urinary protein ($r = 0.417$, $P = 0.022$), and were negatively correlated with estimated glomerular filtration rate ($r = -0.431$, $P = 0.017$). In addition, urinary ANXA1 levels showed a positive correlation with the severity of interstitial fibrosis and tubular atrophy and tubulointerstitial inflammation ($r = 0.405$, $P = 0.026$; and $r = 0.446$, $P = 0.013$, respectively). The level of plasma ANXA1 in DN patients was significantly lower than that in diabetes mellitus patients without kidney involvement (1.22 ± 0.70 vs. 3.64 ± 2.16 ng/ml; $P < 0.001$) and healthy controls (1.22 ± 0.70 vs. 3.20 ± 1.35 ng/ml; $P < 0.001$; Supplementary Figure S7b). However, we did not find any significant correlation between plasma ANXA1 levels and clinical parameters, suggesting that urinary ANXA1/creatinine is a better reflection of kidney inflammation and kidney injuries in DN.

ANXA1 deficiency exacerbates DN in HFD/STZ-treated mice

To determine the role of endogenous ANXA1 in a model of DN, WT and *Anxa1* KO mice were induced to develop DN with HFD/STZ treatment (Figure 2a).

As shown in Supplementary Table S6, diabetic WT mice showed hyperglycemia and hyperlipemia compared with nondiabetic WT mice. Diabetic WT mice displayed increased levels of urine albumin-to-creatinine ratio (uACR), which was further increased significantly in diabetic *Anxa1* KO mice (Figure 2b). Consistent with impaired kidney function, histologic changes, including glomerular size, mesangial matrix expansion, and tubulointerstitial injury, were more severe in diabetic *Anxa1* KO mice than diabetic WT

mice (Figure 2c–f). The glomerular basement membrane thickness and foot process width were also significantly greater in diabetic *Anxa1* KO mice, along with loss of endothelial fenestrations (Figure 2g–j).

Sirius red staining showed an increased deposition of collagen I and III in diabetic WT mice, whereas kidneys from diabetic *Anxa1* KO mice had significantly increased staining, especially in the interstitium and around the vasculature (Figure 2k and l). A similar trend in α-smooth muscle actin accumulation was detected (Figure 2m and n). Moreover, our results showed a significantly higher level of macrophage infiltration in diabetic *Anxa1* KO mice than in diabetic WT mice (Figure 2o and p).

We used polymerase chain reaction array to compare the expression of inflammatory cytokines and receptor genes in kidneys between diabetic *Anxa1* KO and diabetic WT group (Supplementary Table S7). The expression of inflammatory cytokines was significantly upregulated ($P < 0.05$) in diabetic *Anxa1* KO mice, including chemokine (C-C motif) ligand 2, 3, 6, 8, and 20; chemokine receptor 3 and 5; chemokine (C-X-C motif) ligand 1 and 5; interleukin 11, 1β, and 1rn (*Il-11*, *Il-1β*, and *Il-1rn*); secreted phosphoprotein 1 (*Spp1*); and tumor necrosis factor (*Tnf*), compared with diabetic WT mice (Figure 2q). Among these inflammatory cytokine genes, the expression of M1 macrophage markers (*Ccl2*, *Ccl8*, and *Il-1β*) was upregulated significantly in diabetic *Anxa1* KO mice compared with diabetic WT mice, although there was no significant difference in the expression of M2 macrophage markers (*Il-10* and *Ccl24*) between these 2 groups. Moreover, flow cytometry analyses further confirmed that the number of M1 macrophages increased in the kidneys in diabetic *Anxa1* KO mice compared with diabetic WT mice, although the number of M2 macrophages did not have a significant difference between these 2 groups, suggesting that ANXA1 deletion increased M1 polarization in DN (Supplementary Figure S8).

ANXA1 deficiency causes kidney injuries in HFD-treated mice

We utilized the murine model of HFD-induced diabetes to confirm the protective role of ANXA1 in the kidney (Figure 3a). Mice treated with HFD for 4 months presented with obesity, impaired glucose tolerance, and acquired insulin resistance (Supplementary Figure S9). Mice treated with HFD did not develop obvious kidney injury on the C57BL/6J background, as revealed by periodic acid–Schiff staining (Figure 3b–d), which is consistent with the previous studies.[13,14] Ultrastructural analysis demonstrated that HFD-treated *Anxa1* KO mice developed more severe kidney injuries, as evidenced by glomerular basement membrane thickness and podocyte foot process width, compared with the other 3 groups (Figure 3e–g). Podocyte injuries in HFD-treated *Anxa1* KO mice were further confirmed by a significant loss of key podocyte differentiation markers, including nephrin and podocin (Figure 3h–j). In addition, macrophage infiltration marginally increased (Figure 3k and l), and *Il-1β* mRNA levels significantly increased, in diabetic *Anxa1* KO mice compared with diabetic WT mice (Figure 3m). These results further suggested that ANXA1 deficiency may cause kidney injuries in diabetes.

Overexpression of ANXA1 ameliorates DN in HFD/STZ-treated mice

To assess the protective role of endogenous ANXA1, we treated *Anxa1*-Tg mice and WT mice with HFD/STZ to promote kidney injuries of diabetes (Figure 4a). There was no significant difference between diabetic *Anxa1*-Tg mice and diabetic WT mice in blood glucose, body weight, or kidney weight (data not shown). Marked decrease in uACR was observed in diabetic *Anxa1*-Tg mice compared with diabetic WT mice (Figure 4b). HFD/STZ treatment caused increases in glomerular area, mesangial expansion, and tubulointerstitial injuries in WT mice, as revealed by periodic acid–Schiff staining, and the severity of these injuries was markedly attenuated in diabetic *Anxa1*-Tg mice (Figure 4c–e). In addition, HFD/STZ-induced kidney tubulointerstitial fibrosis (Figure 4f–i) and inflammation, including macrophage infiltration (Figure 4j and k) and proinflammatory cytokine expression (Supplementary Figure S10A), were significantly attenuated in *Anxa1*-Tg mice. *Anxa1* overexpression also improved ultrastructural changes, including foot process width and glomerular basement membrane thickness in HFD/STZ-treated mice (Supplementary Figure S10B). These findings suggested that overexpression of *Anxa1* protected the kidney against DN, possibly through regulation of inflammatory and fibrotic processes in the kidney.

Ac2-26 attenuates established nephropathy in a genetic model of diabetes

At the age of 10 weeks, all db/db mice had already developed diabetes, with significantly higher body weight and blood glucose than nondiabetic db/m mice. These diabetic mice also developed significantly higher levels of uACR compared with db/m mice (361.04 ± 83.84 vs. 58.33 ± 4.15 μg/mg; $P < 0.001$; n = 6). To investigate whether Ac2-26 could attenuate established nephropathy in diabetes, we randomly divided db/db mice into treatment arms receiving different doses of Ac2-26. Db/db mice were treated with Ac2-26 for 10 consecutive weeks (Figure 5a). The level of uACR in vehicle-treated db/db mice increased compared with the baseline, whereas Ac2-26 treatment groups presented with significant decrease in uACR compared with the baseline (Figure 5b). In addition, diabetes-induced mesangial matrix expansion and tubulointerstitial injuries were significantly attenuated by Ac2-26 (Figure 5c–e). We assessed kidney inflammation and found an increased level of macrophage infiltration in kidney tissues in vehicle-treated db/db mice compared with vehicle-treated db/m mice. Ac2-26 treatment in db/db mice significantly attenuated the degree of macrophage infiltration, compared with vehicle-treated db/db mice (Figure 5f and g). Furthermore, Ac2-26 treatment groups showed decreased levels of proinflammatory cytokines and chemokines, including *Mcp-1*, *Il-1α*, and *Tnf-α*, in kidneys (Figure 5h–j). Sirius red staining showed that medium and high dose of Ac2-26 treatment could attenuate kidney fibrosis (Figure 5k and l). Transmission electron microscopy analysis showed that Ac2-26 treatment groups alleviated ultrastructural changes, including glomerular basement membrane thickness, podocyte foot process width, and endothelial fenestrations, compared with vehicle-treated db/db mice (Figure 5m–p).

To determine whether an exogenous supply of ANXA1 mimic peptide could reverse the kidney injuries in diabetic *Anxa1* KO mice, Ac2-26 treatment was performed on HFD/STZ-treated diabetic *Anxa1* KO mice. Compared with diabetic *Anxa1* KO mice without Ac2-26 administration, diabetic *Anxa1* KO mice with Ac2-26 administration had significant

improvements in albuminuria and kidney pathologic changes (Supplementary Figure S11). These results were consistent with the above-mentioned data of the protective effect of Ac2-26 treatment in db/db mice.

Collectively, these data suggested that Ac2-26 administration could attenuate kidney injuries in diabetes.

ANXA1 binds to the p65 subunit of NF-κB and inhibits its activation in HK-2 cells

Because we found that ANXA1 colocalized with the tubular epithelial cell in kidney specimens of DN patients, we stimulated proximal tubular epithelial HK-2 cells with high glucose plus palmitic acid (HGPA) to simulate the *in vivo* environment of diabetes. Compared with HK-2 cells without treatment, the *ANXA1* mRNA expression increased in cells exposed to HGPA (Supplementary Figure S12). *ANXA1* knockdown (small, interfering RNA [siRNA] against ANXA1 [si*ANXA1*]) could upregulate the proinflammatory factors in response to HGPA treatment, including *IL-1β*, *TGF-β*, and *TNF* (Figure 6a–c).

The transcription factor NF-κB plays an important role in the process of inflammation.[15,16] Western blot analysis suggested that si*ANXA1* led to an increase in the expression of NF-κB phosphorylated p65 in HK-2 cells treated with HGPA (Figure 6d), consistent with the *in vivo* results in mouse models (Supplementary Figure S13). However, the phosphorylation level of IκBα was not significantly increased in si*ANXA1* group treated with HGPA compared with negative control siRNA group treated with HGPA (Supplementary Figure S14). To explore the binding of ANXA1 and p65, we performed coimmunoprecipitation of ANXA1 and p65 in HK-2 cells as well as in kidney tissues of HFD/STZ WT mice. The results showed that ANXA1 physically interacted with p65 both *in vitro* and *in vivo* (Figure 6e and Supplementary Figure S15). Moreover, surface plasmon resonance analysis demonstrated that ANXA1 exhibited a high binding affinity for p65 (equilibrium dissociation constant [KD] = 1.299×10^{-8} mol/L; Figure 6f). To determine whether there was any functional consequence to the coexpression, the electrophoretic mobility shift assay test was performed using nuclear extracts from HK-2 cells. As shown in Figure 6g, HGPA increased the binding of NF-κB to the κB probe. Compared with the negative control siRNA group treated with HGPA, the binding activity of NF-κB to the κB oligomer was higher in the si*ANXA1* group treated with HGPA. Consistent with the electrophoretic mobility shift assay analysis, the NF-κB activity, assessed by enzyme-linked immunosorbent assay, was significantly increased in the si*ANXA1* group treated with HGPA compared with negative control siRNA group treated with HGPA (Figure 6h). Altogether, these findings suggested that ANXA1 could associate with p65 to prevent p65 phosphorylation and NF-κB activation in HK-2 cells.

In addition, we explored the potential protection of ANXA1 mimetic peptide Ac2-26 in HK-2 cells. We found Ac2-26 (15 μmol/L) decreased HGPA-induced cytokine release (Supplementary Figure S16A). Ac2-26, as an exogenous administration of peptide, is not able to cross the cell membrane and is thus unlikely to bind to NF-κB p65, like ANXA1 protein, which was consistent with surface plasmon resonance analysis (Supplementary Figure S16B). To determine the potential pharmacologic targeting of Ac2-26, lipoxin A(4)/formyl peptide receptor 2 (ALX/FPR2) selective antagonist Trp-Arg-Trp-Trp-Trp-Trp

(WRW4), selective FPR1 antagonist N-(tert-butoxycarbonyl)-Met-Leu-Phe (Boc-MLF) (1 μmol/L), or pan-FPR antagonist Boc-MLF (10 μmol/L) was added before Ac2-26 and HGPA. We found that it was mainly FPR1, not ALX/FPR2, that plays the role of mediating Ac2-26 effects on proresolution in HK-2 cells (Supplementary Figure S16A). We found that the NF-κB activation increased in HK-2 cells treated with HGPA compared with that without HGPA. However, HGPA-triggered NF-κB activation was reduced by Ac2-26 treatment (Supplementary Figure S16C).

DISCUSSION

Over the last decade, numerous studies have demonstrated that inflammation is involved in the cascade of events that lead to DN.[17] Therefore, promoting the resolution of inflammation is a potential therapeutic approach for alleviating diabetes and its complications.[18] ANXA1 promotes the production of anti-inflammatory cytokine interleukin-10 and plays an important role in the resolution of inflammation.[19] Although numerous studies have focused on the profitable role of ANXA1 in disease statuses, the role of ANXA1 in DN is not yet fully clear. Herein, we identified upregulation of ANXA1 in kidneys of DN patients and reported the correlation between the level of ANXA1 in kidneys and kidney function as well as kidney outcomes in independent cohorts for the first time. We further evaluated the potential role of ANXA1 in DN, showing that genetic ablation of *Anxa1* exacerbated kidney injury and overexpression of *Anxa1* ameliorated kidney injury in DN mice. In addition to endogenous ANXA1, we evaluated the therapeutic potential of Ac2-26 (ANXA1 mimetic peptide) for DN. Finally, we demonstrated the corresponding protective mechanisms of ANXA1 in tubular epithelial cells *in vitro*.

In the present study, we detected ANXA1 in protein levels and *ANXA1* mRNA levels in kidneys in different DN cohorts and characterized the expression profile of ANXA1 in various types of cells in kidneys. The expression of ANXA1 in kidneys was increased in patients with DN compared with healthy controls. Moreover, there was a significant negative correlation between the level of ANXA1 in kidneys and renal function. These data suggested that in the context of DN, the upregulation of ANXA1 in kidneys may be a possible attempt to attenuate the local inflammatory response. However, we found glomerular ANXA1 negatively correlated with glomerulosclerosis. It may be caused by a decrease in glomerular cells and an increased accumulation of extracellular matrix during the progression of glomerulosclerosis in DN.[20,21] We found that plasma ANXA1 level was decreased in DN patients. ANXA1 is mainly produced by a variety of immune cells, including monocytes, macrophages, and neutrophils.[22,23] DN is characterized by the infiltration of macrophages and the increased production of cytokines in kidneys. The decrease of circulating ANXA1 in DN may be caused by the increase of ANXA1 in the target inflammatory sites (i.e., kidneys). A similar phenomenon was also found in exacerbated asthmatics.[24] In addition, we demonstrated that renal epithelial cells, including podocytes and tubular cells, also secreted ANXA1 in response to kidney inflammation. Moreover, we found that the urinary level of ANXA1 was increased, and there was a significant correlation between urinary ANXA1 and tubulointerstitial injuries in DN. Ka *et al.* found that the urinary ANXA1 was detectable as early as the stage of normoalbuminuria in diabetes mellitus patients.[25] Based on the previous studies and our data, we speculate that ANXA1 may enter the urine by either secretion

from renal epithelial cells or direct release from immune cells. However, the results did not exclude the possibility that some of the excreted ANXA1 may be derived from glomerular filtration.

Our studies further explored the functional role of ANXA1 in DN mouse models. We found that *Anxa1* KO worsened diabetes-induced kidney injury. These findings suggested that once there was *Anxa1* deficiency, proresolving activities were obviously insufficient to counteract proinflammatory signaling in HFD/STZ diabetic model, leading to persistent inflammation and more severe kidney injury. Moreover, flow cytometry and polymerase chain reaction array results suggested that ANXA1 could influence macrophage polarization. Lack of ANXA1 is able to lead to an increase of M1 macrophages and aggravation of inflammation in kidneys in DN, which is consistent with the previous study.[26] In addition, our results showed that overexpression of *Anxa1* alleviated HFD/STZ-induced kidney injury, suggesting the proresolving activation mediated by ANXA1 could counteract the proinflammatory response.

To further explore the therapeutic effects of exogenous ANXA1, db/db mice were administrated different doses of Ac2-26.[27] Treatment with Ac2-26 is considered to have fewer adverse effects due to its ability to mimic or induce natural pathways mediating the resolution of inflammation.[28] Renoprotective effects were observed in db/db mice administered Ac2-26. Consistently, we also found the protective effects of Ac2-26 in diabetic *Anxa1* KO mice.

In the present study, we further found that *ANXA1* knockdown could upregulate the proinflammatory and profibrotic factors *in vitro*, showing ANXA1 could directly target renal tubular epithelial cells in kidneys to prevent the injury from HGPA stimulation. In addition to the well-recognized pathway of extracellular ANXA1 binding to FPRs,[29] intracellular ANXA1 associating with NF-κB to suppress its transcriptional activity in cancer cells could be of relevance.[30] Because NF-κB is one of the crucial transcription factors relevant to the progression of DN,[15,16] we assessed whether intracellular ANXA1 plays a role in DN by modulating NF-κB activity. Both *in vitro* and *in vivo* studies showed the interactions between ANXA1 and p65, and the binding of ANXA1 to NF-κB further inhibited the activation of NF-κB signaling. Somewhat surprisingly, the phosphorylation levels of IκBα were not altered significantly after ANXA1 silencing. Thus, we proposed that ANXA1 interacts with p65 and inhibits its phosphorylation, instead of affecting the degradation of IκBs and the release of p65 (i.e., ANXA1 affects the downstream IκBα degradation). Consistent with this hypothesis, increased phosphorylated p65 was observed in si*ANXA1* group treated with HGPA compared with negative control siRNA group treated with HGPA.

According to the comprehensive work by Purvis *et al.*, *Anxa1* gene deletion in mice treated with HFD led to severe diabetic phenotype. It was reported that ANXA1 could protect against excessive mitochondrial proton leak by activating ALX/FPR2 under hyperglycemic conditions in human hepatocytes.[5] Another study from the same group demonstrated that *Anxa1* KO aggravated kidney injuries in STZ-induced mouse model of type 1 diabetes by regulating v-akt murine thymoma viral oncogene homolog (Akt) signaling.[6] The current study further confirmed ANXA1 in restricting kidney inflammation in DN. Moreover, we

simulated the *in vivo* environment of diabetes and explored the direct role of intracellular ANXA1 in renal tubular epithelial cells.

In conclusion, our findings demonstrate that endogenous ANXA1 protects against nephropathy in diabetes. Intracellular ANXA1 may suppress NF-κB signaling to modulate kidney inflammation in DN. Our preclinical studies suggest that ANXA1 may be a promising therapeutic approach to treat DN. These observations also indicate that promoting endogenous resolution of inflammation may be an effective therapeutic paradigm for DN.

Supplementary Material

Refer to Web version on PubMed Central for supplementary material.

ACKNOWLEDGEMENTS

SE reports grants from National Institutes of Health (NIH)–National Institute of Diabetes and Digestive and Kidney Diseases (NIDDK) and National Center for Advancing Translational Sciences, during the conduct of the study. MK reports grants from the NIH during the conduct of the study. This study is supported by a grant from National Key Research and Development Program (no. 2016YFC1305405), grants from the National Natural Science Foundation (nos. 82090021, 82070748, 91639108, 81770272, and 81970425), a grant from Interdisciplinary Clinical Research Project of Peking University First Hospital, a grant by the University of Michigan Health System and Peking University Health Sciences Center Joint Institute for Translational and Clinical Research (no. BMU2017JI001), a grant from Peking University Medicine Seed Fund for Interdisciplinary Research (no. BMU2018MX025), and Innovation Fund for Outstanding Doctoral Candidates of Peking University Health Science Center (no. 71013Y2029). Additional support was provided by the Applied Systems Biology Core at the University of Michigan George M. O'Brien Kidney Translational Core Center (P30 DK081943) and by the Intramural Research Program of the NIDDK.

DISCLOSURE

SE reports grants from AstraZeneca, Gilead Sciences, NovoNordisk, Janssen, and Eli Lilly and Company, outside the submitted work. MK reports nonfinancial support from University of Michigan during the conduct of the study; grants from JDRF, AstraZeneca, NovoNordisk, Eli Lilly, Gilead, Goldfinch Bio, Merck, Janssen, Boehringer-Ingelheim, Moderna, European Union Innovative Medicine Initiative, Chan Zuckerberg Initiative, Certa, Chinook, amfAR, Angion Pharmaceuticals, RenalytixAI, Travere Therapeutics, Regeneron, and IONIS Pharmaceuticals; other from Astellas; other from Poxel; and grants from Shire; outside the submitted work. In addition, MK has a licensed patent PCT/EP2014/073413, "Biomarkers and Methods for Progression Prediction for Chronic Kidney Disease." WJ has a licensed patent PCT/EP2014/073413, "Biomarkers and Methods for Progression Prediction for Chronic Kidney Disease." All the other authors declared no competing interests.

REFERENCES

1. Pradhan AD, Manson JE, Rifai N, et al. C-reactive protein, interleukin 6, and risk of developing type 2 diabetes mellitus. JAMA. 2001;286:327–334. [PubMed: 11466099]
2. Hu FB, Meigs JB, Li TY, et al. Inflammatory markers and risk of developing type 2 diabetes in women. Diabetes. 2004;53:693–700. [PubMed: 14988254]
3. Serhan CN, Yacoubian S, Yang R. Anti-inflammatory and proresolving lipid mediators. Annu Rev Pathol. 2008;3:279–312. [PubMed: 18233953]
4. Flower RJ, Blackwell GJ. Anti-inflammatory steroids induce biosynthesis of a phospholipase A2 inhibitor which prevents prostaglandin generation. Nature. 1979;278:456–459. [PubMed: 450050]
5. Purvis GSD, Collino M, Loiola RA, et al. Identification of AnnexinA1 as an endogenous regulator of RhoA, and its role in the pathophysiology and experimental therapy of type-2 diabetes. Front Immunol. 2019;10:571. [PubMed: 30972066]
6. Purvis GSD, Chiazza F, Chen J, et al. Annexin A1 attenuates microvascular complications through restoration of Akt signalling in a murine model of type 1 diabetes. Diabetologia. 2018;61:482–495. [PubMed: 29085990]

7. Panda SK, Wefers B, Ortiz O, et al. Highly efficient targeted mutagenesis in mice using TALENs. Genetics. 2013;195:703–713. [PubMed: 23979585]
8. Li Z, Michael IP, Zhou D, et al. Simple piggyBac transposon-based mammalian cell expression system for inducible protein production. Proc Natl Acad Sci U S A. 2013;110:5004–5009. [PubMed: 23476064]
9. Tervaert TW, Mooyaart AL, Amann K, et al. Pathologic classification of diabetic nephropathy. J Am Soc Nephrol. 2010;21:556–563. [PubMed: 20167701]
10. Wu P, Wang Y, Davis ME, et al. Store-operated Ca^{2+} channels in mesangial cells inhibit matrix protein expression. J Am Soc Nephrol. 2015;26:2691–2702. [PubMed: 25788524]
11. Kelly DJ, Wilkinson-Berka JL, Allen TJ, et al. A new model of diabetic nephropathy with progressive renal impairment in the transgenic (mRen-2)27 rat (TGR). Kidney Int. 1998;54:343–352. [PubMed: 9690200]
12. Nair V, Komorowsky CV, Weil EJ, et al. A molecular morphometric approach to diabetic kidney disease can link structure to function and outcome. Kidney Int. 2018;93:439–449. [PubMed: 29054530]
13. Breyer MD, Böttinger E, Brosius FC, et al. Mouse models of diabetic nephropathy. J Am Soc Nephrol. 2005;16:27–45. [PubMed: 15563560]
14. Brosius FC, Alpers CE, Bottinger EP, et al. Mouse models of diabetic nephropathy. J Am Soc Nephrol. 2009;20:2503–2512. [PubMed: 19729434]
15. Sanchez AP, Sharma K. Transcription factors in the pathogenesis of diabetic nephropathy. Expert Rev Mol Med. 2009;11:e13. [PubMed: 19397838]
16. Schmid H, Boucherot A, Yasuda Y, et al. Modular activation of nuclear factor-kappaB transcriptional programs in human diabetic nephropathy. Diabetes. 2006;55:2993–3003. [PubMed: 17065335]
17. Navarro-González JF, Mora-Fernández C, Muros de Fuentes M, et al. Inflammatory molecules and pathways in the pathogenesis of diabetic nephropathy. Nat Rev Nephrol. 2011;7:327–340. [PubMed: 21537349]
18. Brennan EP, Mohan M, McClelland A, et al. Lipoxins regulate the early growth response-1 network and reverse diabetic kidney disease. J Am Soc Nephrol. 2018;29:1437–1448. [PubMed: 29490938]
19. Ferlazzo V, D'Agostino P, Milano S, et al. Anti-inflammatory effects of annexin-1: stimulation of IL-10 release and inhibition of nitric oxide synthesis. Int Immunopharmacol. 2003;3:1363–1369. [PubMed: 12946433]
20. Ziyadeh FN, Wolf G. Pathogenesis of the podocytopathy and proteinuria in diabetic glomerulopathy. Curr Diabetes Rev. 2008;4:39–45. [PubMed: 18220694]
21. Nakagawa T, Sato W, Glushakova O, et al. Diabetic endothelial nitric oxide synthase knockout mice develop advanced diabetic nephropathy. J Am Soc Nephrol. 2007;18:539–550. [PubMed: 17202420]
22. Perretti M, Croxtall JD, Wheller SK, et al. Mobilizing lipocortin 1 in adherent human leukocytes downregulates their transmigration. Nat Med. 1996;2:1259–1262. [PubMed: 8898757]
23. Oliani SM, Damazo AS, Perretti M. Annexin 1 localisation in tissue eosinophils as detected by electron microscopy. Mediators Inflamm. 2002;11:287–292. [PubMed: 12467520]
24. Lee SH, Lee PH, Kim BG, et al. Annexin A1 in plasma from patients with bronchial asthma: its association with lung function. BMC Pulm Med. 2018;18:1. [PubMed: 29301525]
25. Ka SM, Tsai PY, Chao TK, et al. Urine annexin A1 as an index for glomerular injury in patients. Dis Markers. 2014;2014:854163. [PubMed: 24591769]
26. McArthur S, Juban G, Gobbetti T, et al. Annexin A1 drives macrophage skewing to accelerate muscle regeneration through AMPK activation. J Clin Invest. 2020;130:1156–1167. [PubMed: 32015229]
27. Perretti M, Dalli J. Exploiting the Annexin A1 pathway for the development of novel anti-inflammatory therapeutics. Br J Pharmacol. 2009;158:936–946. [PubMed: 19845684]
28. Li C, Zhao Y, Cheng J, et al. A proresolving peptide nanotherapy for site-specific treatment of inflammatory bowel disease by regulating proinflammatory microenvironment and gut microbiota. Adv Sci. 2019;6: 1900610.

29. Ansari J, Kaur G, Gavins FNE. Therapeutic potential of Annexin A1 in ischemia reperfusion injury. Int J Mol Sci. 2018;19:1211.

30. Zhang Z, Huang L, Zhao W, et al. Annexin 1 induced by anti-inflammatory drugs binds to NF-kappaB and inhibits its activation: anticancer effects in vitro and in vivo. Cancer Res. 2010;70:2379–2388. [PubMed: 20215502]

Translational Statement

Diabetic nephropathy (DN) is the leading cause of end-stage kidney disease worldwide. Novel strategies for DN therapy are needed urgently. Our data demonstrate that annexin A1 (ANXA1), as a proresolving molecule, is a promising therapeutic target for treating DN. We show that ANXA1 deficiency exacerbates kidney injuries in DN, whereas ANXA1 overexpression or treatment with Ac2-26, an ANXA1 mimetic peptide, protects against the progression of DN by reducing kidney tubular injuries, kidney inflammation, and fibrosis. Our findings suggest a potential therapeutic approach based on inflammation resolution to treat DN effectively.

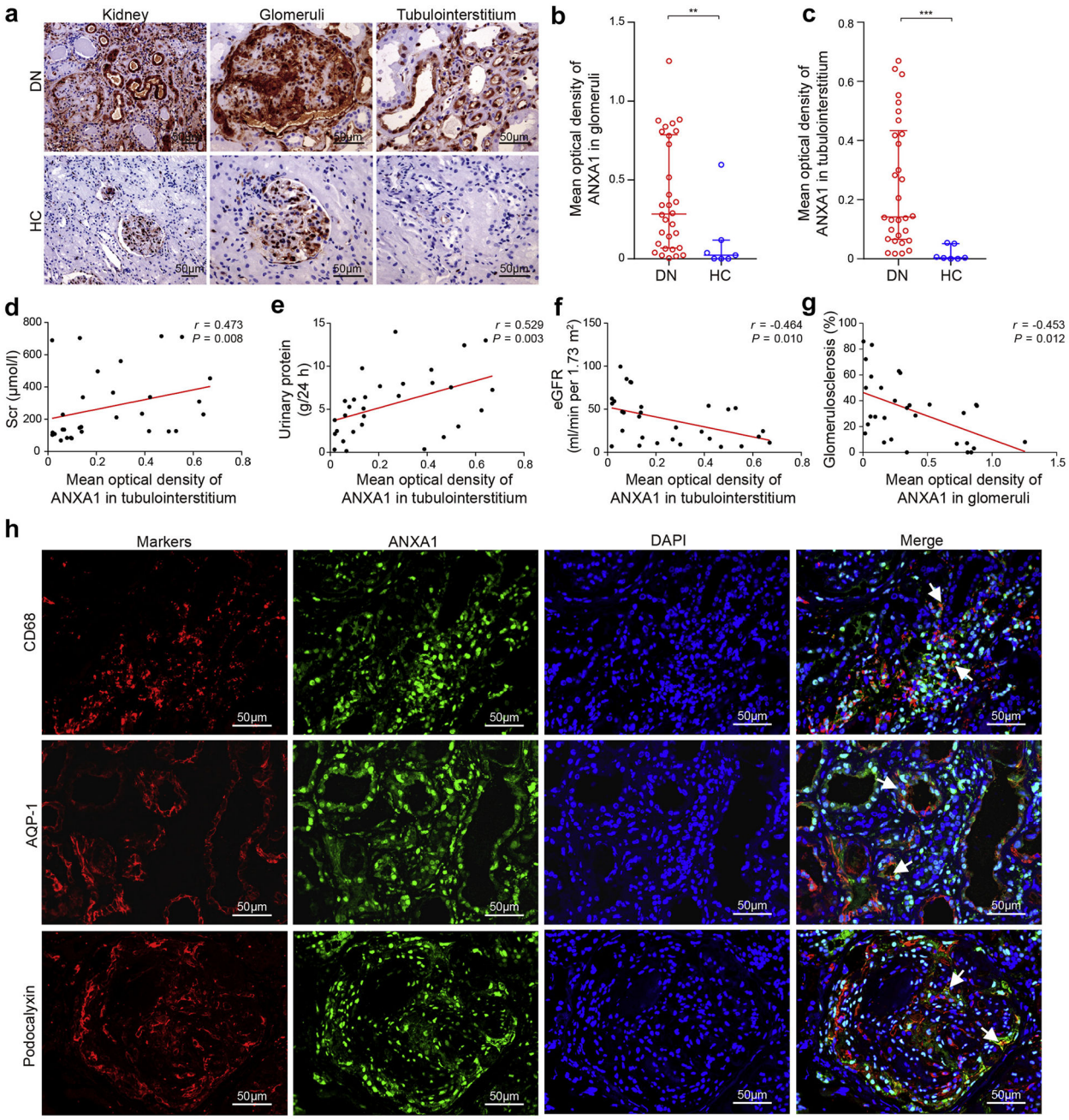

Figure 1 |. Annexin A1 (ANXA1) in kidney biopsies from patients with diabetic nephropathy (DN).

(**a**) Representative images of ANXA1 staining in human kidney cortical tissue, in the glomeruli and tubulointerstitium from DN and control in the Chinese cohort. Bars = 50 μm. (**b**) Glomerular ANXA1 staining in DN patients (n = 30) was significantly higher than that in controls (n = 7). (**c**) Tubulointerstitial ANXA1 staining in DN patients (n = 30) was significantly higher than that in controls (n = 7). Tubulointerstitial ANXA1 expression was positively correlated with (**d**) serum creatinine (Scr) and (**e**) 24-hour urinary protein in DN patients. (**f**) Tubulointerstitial ANXA1 expression was negatively correlated with estimated

glomerular filtration rate (eGFR) in DN patients. (**g**) Glomerular ANXA1 expression was negatively correlated with the percentage of glomerulosclerosis. (**h**) Representative confocal microscopic images showed the expression of ANXA1 in macrophages (cluster of differentiation [CD] 68), proximal tubule epithelial cells (aquaporin 1 [AQP-1]), and podocytes (podocalyxin) in kidneys from DN. Bars = 50 μm. Data analyses were performed by Mann-Whitney *U* test for 2 groups. Correlations were determined by Spearman analysis. Data are expressed as median (interquartile range). $^{**}P < 0.01$, and $^{***}P < 0.001$. DAPI, 4′,6-diamidino-2-phenylindole; HC, healthy control. To optimize viewing of this image, please see the online version of this article at www.kidney-international.org.

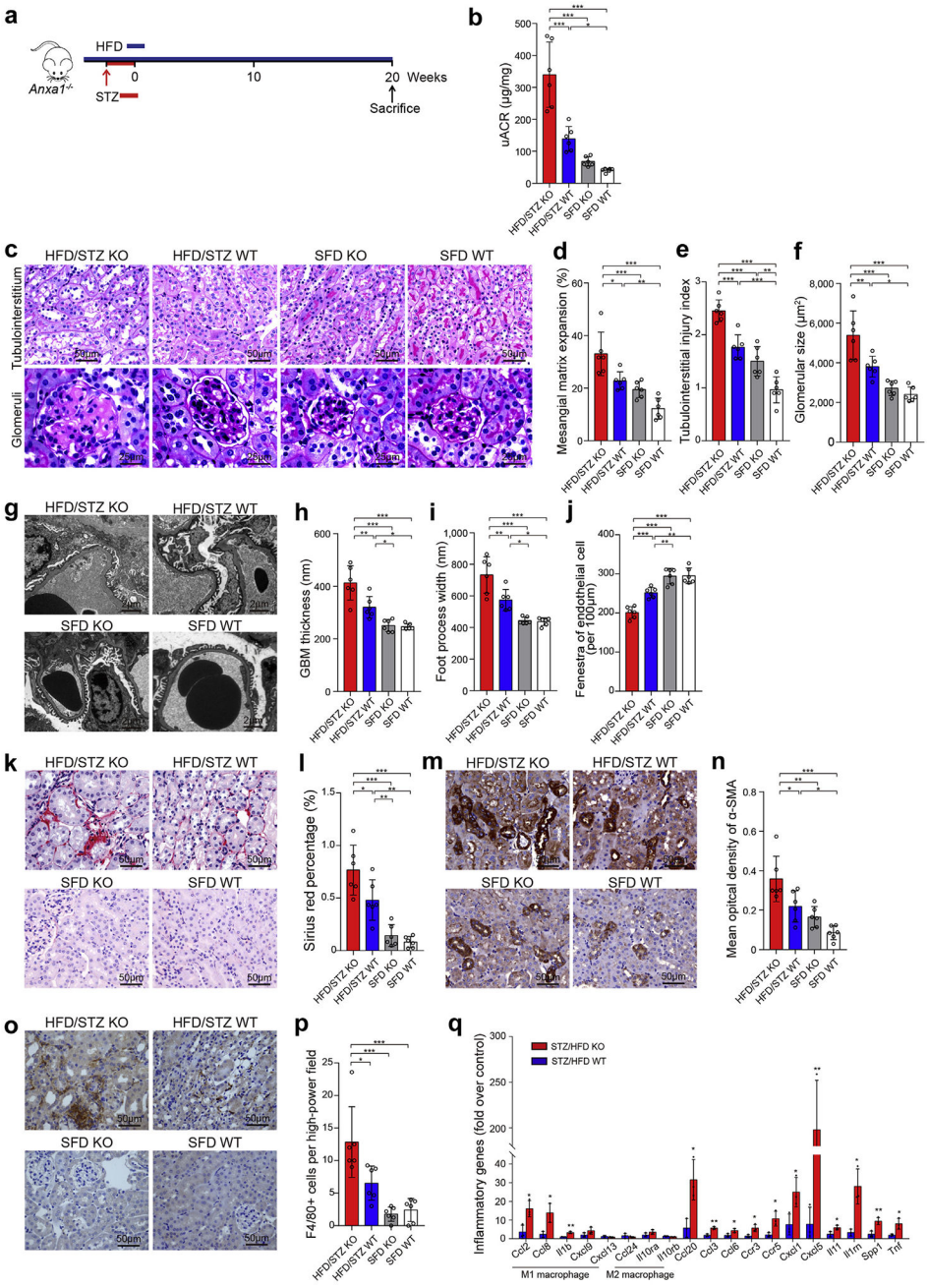

Figure 2 |. Annexin A1 (*Anxa1*) knockout (KO) aggravated nephropathy in high-fat diet (HFD) plus streptozotocin (STZ)-induced diabetic nephropathy mice.

(**a**) Study design overview. Eight-week-old *Anxa1* KO mice were fed with an HFD for 1 month, followed by i.p. injection of 50 mg/kg STZ for 5 days. Mice were maintained for 20 weeks of HFD feeding before sacrifice. n = 6 per group. (**b**) Four groups were evaluated for urine albumin-to-creatinine ratio (uACR). (**c**) Representative photomicrographs of periodic acid–Schiff staining. Bar = 50 μm for tubulointerstitium and 25 μm for glomeruli. Quantification showing (**d**) mesangial matrix expansion, (**e**) tubulointerstitial injury index, and (**f**) glomerular size. (**g**) Representative photomicrographs of transmission electron

microscopy. Bars = 2 μm. Quantification of (**h**) mean glomerular basement membrane (GBM) thickness, (**i**) mean foot process width, and (**j**) endothelial fenestrations in 4 groups. (**k**) Representative photomicrographs of Sirius red. Bars = 50 μm. (**l**) Quantitative analysis of Sirius red. (**m**) Representative photomicrographs of α-smooth muscle actin (α-SMA). Bars = 50 μm. (**n**) Quantitative analysis of α-SMA. (**o**) Representative photomicrographs of F4/80 staining. Bars = 50 μm. (**p**) Quantitative analysis of F4/80 staining. (**q**) Quantification of inflammatory gene expression by polymerase chain reaction array, HFD/STZ *Anxa1* KO versus HFD/STZ wild-type (WT) mice (n = 3). Throughout, data analyses were performed by Student *t* test for 2 groups and 2-way analysis of variance, followed by a Tukey test, for 4 groups. Data are expressed as mean ± SD. **P* < 0.05, ***P* < 0.01, and ****P* < 0.001. SFD, standard fat diet. To optimize viewing of this image, please see the online version of this article at www.kidney-international.org.

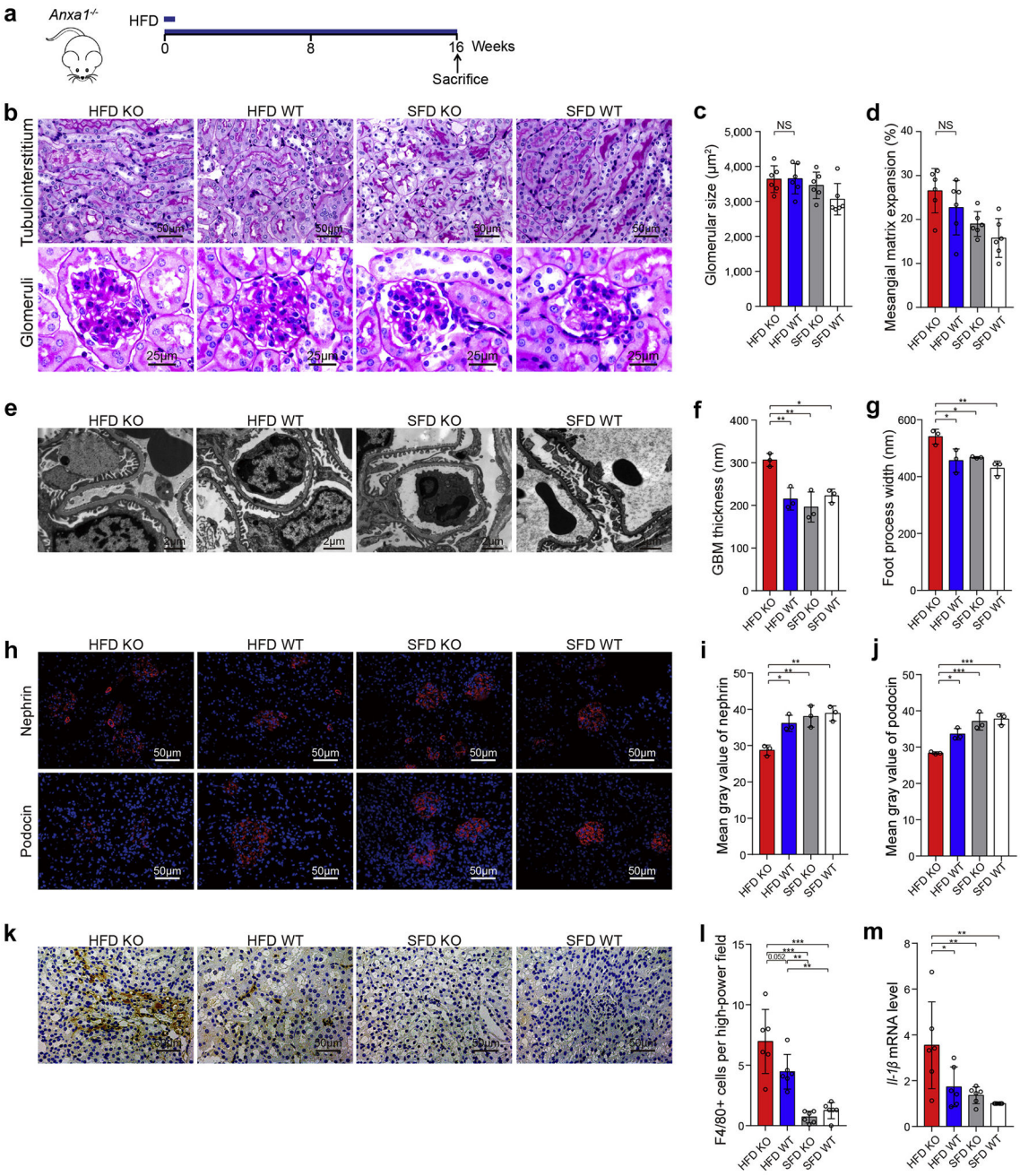

Figure 3 |. Annexin A1 (*Anxa1*) knockout (KO) caused kidney injuries in high-fat diet (HFD)–induced diabetic mice.

(**a**) Study design overview. *Anxa1* KO mice were maintained for 16 weeks of HFD feeding. (**b**) Representative photomicrographs showing typical tubulointerstitial (bars = 50 μm) and glomerular structure (bars = 25 μm) in control and diabetic mice. Quantification showing (**c**) glomerular size and (**d**) mesangial matrix expansion (n = 6). (**e**) Representative transmission electron microscopy images in kidney cortex tissue isolated from diabetic *Anxa1* KO and wild-type (WT) mice as well as nondiabetic mice. Bars = 2 μm. Quantification of (**f**) mean glomerular basement membrane (GBM) thickness and (**g**) mean foot process width in 4

groups (n = 3). (**h**) Representative microscopic images showing the expressions of nephrin and podocin in the kidney from different groups of mice. Bars = 50 μm. Quantitative analysis of (**i**) nephrin and (**j**) podocin (n = 3). (**k**) Representative photomicrographs of F4/80 staining. Bars = 50 μm. (**l**) Quantitative analysis of F4/80 staining. (**m**) Quantification of *Il-1β* gene expression by real-time polymerase chain reaction among 4 groups (n = 6). Throughout, data analyses were performed by 2-way analysis of variance, followed by a Tukey test, for 4 groups and expressed as mean ± SD. $*P < 0.05$, $**P < 0.01$, and $***P < 0.001$. SFD, standard fat diet. To optimize viewing of this image, please see the online version of this article at www.kidney-international.org.

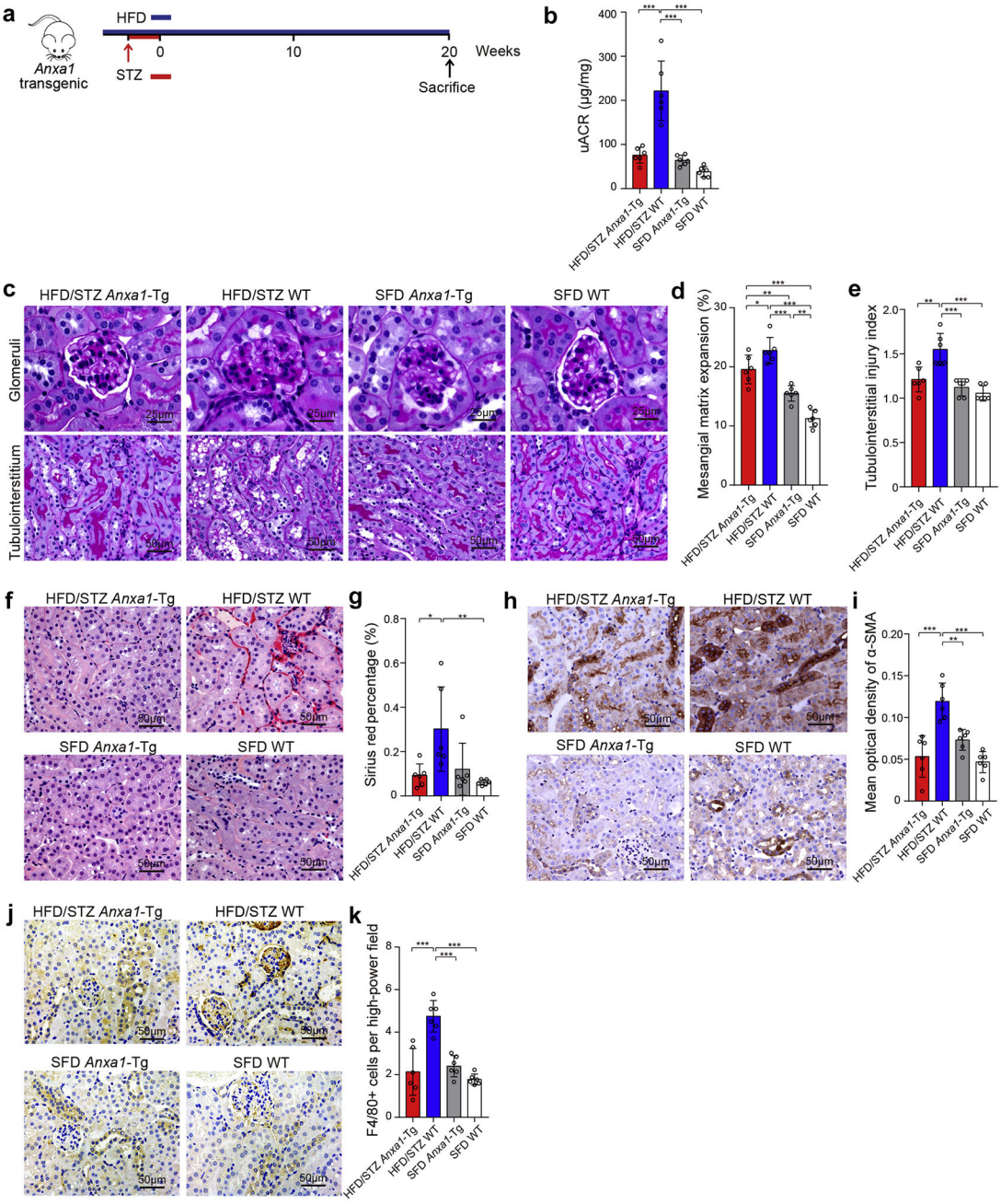

Figure 4 |. Overexpression of annexin A1 (*Anxa1*) suppresses diabetic nephropathy.

(**a**) Study design overview. *Anxa1* transgenic (*Anxa1*-Tg) mice and wild-type (WT) mice were fed with a high-fat diet (HFD) for 1 month, followed by a daily i.p. injection of 50 mg/kg streptozotocin (STZ) for 5 days. Mice were maintained for 20 weeks on an HFD before sacrifice. n = 6 per group. (**b**) Urine albumin-to-creatinine ratio (uACR) in 4 groups. (**c**) Representative photomicrographs of periodic acid–Schiff staining. Bars = 50 μm for tubulointerstitium and 25 μm for glomeruli. Quantification showing (**d**) mesangial matrix expansion and (**e**) tubulointerstitial injury index. (**f**) Representative photomicrographs of Sirius red. Bars = 50 μm. (**g**) Quantitative analysis of Sirius red. (**h**) Representative

photomicrographs of α-smooth muscle actin (α-SMA). Bars = 50 μm. (**i**) Quantitative analysis of α-SMA. (**j**) Representative photomicrographs of F4/80 staining. Bars = 50 μm. (**k**) Quantitative analysis of F4/80 staining. Data represent mean ± SD. Data analyses were performed by 2-way analysis of variance, followed by a Tukey test, for 4 groups. $*P < 0.05$, $**P < 0.01$, and $***P < 0.001$. SFD, standard fat diet. To optimize viewing of this image, please see the online version of this article at www.kidney-international.org.

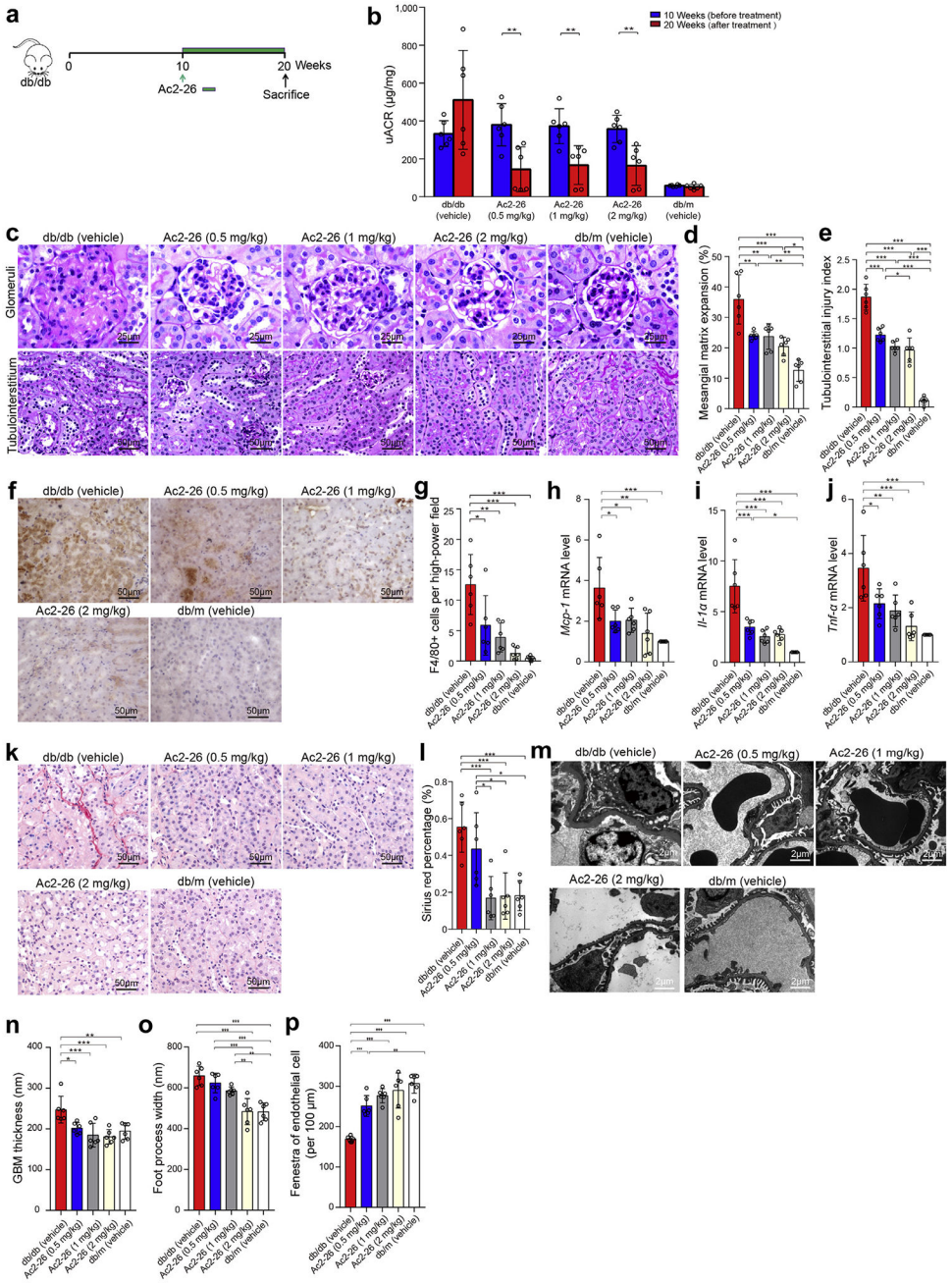

Figure 5 |. Ac2-26 administration treats established nephropathy in db/db mice.

(**a**) Ac2-26 treatment protocol for db/db mice. Diabetic db/db mice were allowed to progress for 10 weeks, after which the subgroups of diabetic mice were administered different concentrations of Ac2-26 (0.5, 1, or 2 mg/kg), or phosphate-buffered saline every 2 days i.p. from weeks 10 to 20. n = 6 per group. (**b**) The levels of urine albumin-to-creatinine ratio (uACR) at 10 and 20 weeks (n = 6). (**c**) Representative photomicrographs of periodic acid–Schiff staining. Bars = 50 μm for tubulointerstitium and 25 μm for glomeruli. Quantification showing (**d**) mesangial matrix expansion and (**e**) tubulointerstitial injury index. (**f**) Representative photomicrographs of F4/80 staining. Bars = 50 μm. (**g**)

Quantitative analysis of F4/80 staining. Quantification of (**h**) *Mcp-1*, (**i**) *Il-1*α, and (**j**) *Tnf-α* gene expression by real-time polymerase chain reaction among 4 groups. (**k**) Representative photomicrographs of Sirius red. Bars = 50 μm. (**l**) Quantitative analysis of Sirius red. (**m**) Representative transmission electron microscopy images. Bars = 2 μm. Quantification of (**n**) mean glomerular basement membrane (GBM) thickness, (**o**) foot process width, and (**p**) endothelial fenestrations (n = 6). Data analyses were performed by Student *t* test for 2 groups and 1-way analysis of variance, followed by a Tukey test, for multiple groups. $*P < 0.05$, $**P < 0.01$, and $***P < 0.001$. To optimize viewing of this image, please see the online version of this article at www.kidney-international.org.

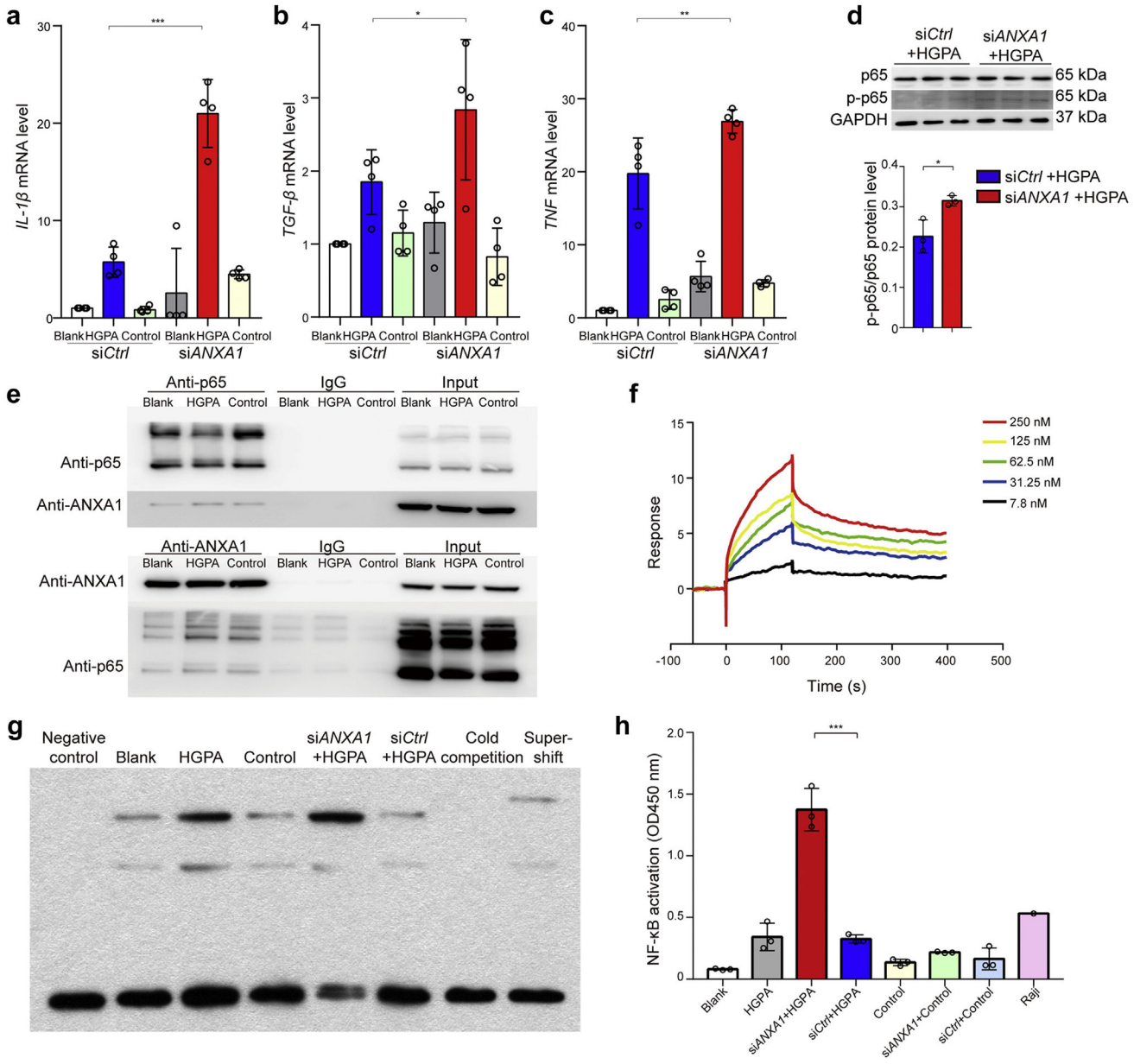

Figure 6 |. Annexin A1 (ANXA1) binds to the p65 subunit of nuclear factor (NF)–κB and inhibits its activation in HK-2 cells.

Quantitative real-time polymerase chain reaction analyzed (**a**) *Il-1β*, (**b**) *TGF-β*, and (**c**) *TNF* mRNA level in HK-2 cells transfected with *ANXA1* small, interfering RNA (siRNA) under high glucose plus palmitic acid (HGPA) conditions. n = 4 per group. (**d**) Top: Representative Western blot images. Bottom: Analyses of phosphorylated p65 (p-p65) and p65 in HK-2 cells with treatment. n = 3 per group. (**e**) Top: Total protein lysates of HK-2 cells treated with HGPA or siRNA against ANXA1 (si*ANXA1*) were immunoprecipitated using an antibody against the p65 subunit of NF-κB and immunoblotted (IB) against ANXA1. Bottom: Total protein lysates of HK-2 cells treated with HGPA or si*ANXA1* were immunoprecipitated using an antibody against ANXA1 and IB against the p65 subunit of NF-κB. (**f**) The surface plasmon resonance (SPR) curves generated from ANXA1 binding

to p65. The ANXA1 protein concentration ranged from 7.8 to 250 nM. The apparent dissociation constants for the interaction were obtained from fitting the SPR response curves to a simple 1:1 Langmuir binding model. (**g**) Electrophoretic mobility shift assay showed the binding of NF-κB to the DNA probe in HK-2 cells under different treatments. (**h**) Enzyme-linked immunosorbent assay showed the NF-κB activity as indicated. n = 3 per group. Data analysis was performed by Student *t* test for 2 groups and 2-way analysis of variance, followed by a Tukey test, for multiple groups and expressed as mean ± SD. The blank group served as the normal control group. The control group served as the isotonic solvent control group using mannitol and endotoxin-free bovine serum albumin. $*P < 0.05$, $**P < 0.01$, and $***P < 0.001$. GAPDH, glyceraldehyde 3-phosphate dehydrogenase; si*Ctrl*, negative control siRNA.